

MESONIC CORRELATORS IN HOT QCD

M. LAINE

*Faculty of Physics, University of Bielefeld,
D-33501 Bielefeld, Germany*

E-mail: laine@physik.uni-bielefeld.de

Certain spacelike mesonic correlation lengths serve as interesting theoretical probes for the reliability of perturbation theory in high-temperature QCD, are directly sensitive to chiral symmetry restoration and to the axial anomaly, and might also have indirect phenomenological signatures in idealised heavy ion collision experiments. I review here the weak-coupling predictions for some of these correlation lengths, to be compared with results from lattice Monte Carlo simulations.

1. Introduction

At a finite temperature T , Lorentz symmetry is broken by the heat bath, so that temporal and spatial directions are, in general, unrelated. Correlation functions in the (Minkowski) time direction can be used to define, after a Fourier transform, spectral functions for various operators, and the spectral functions in turn determine fundamental “real-time” properties of the plasma, such as particle production rates.¹ These are then directly measurable in heavy ion collision experiments (modulo problems with background contamination, etc).

Correlation functions in spatial directions, in contrast, address questions such as: At which length scales are thermal fluctuations correlated? At which length scales are external charges screened? In principle these “static” observables are also physical and may lead to detectable signals, however in practice the relations are indirect and therefore weaker than for real-time observables. On the other hand, static quantities are eminently suited to measurements in *lattice experiments*. Lattice simulations will hence be the most immediate “phenomenological” reference point in the following.

There is naturally a vast variety of different operators that can be correlated. The operators can be classified according to their discrete and continuous global symmetry properties, leading to many independent cor-

relation lengths. The analytic structures of various purely *gluonic* correlators were discussed in Ref. 2, and the corresponding lattice measurements are rather precise by now.^{3–8} The purpose of this talk is to analyse the structures of *mesonic* correlators, for which the status has been somewhat less advanced. This talk is based on the original study in Ref. 9.

2. Detailed setup

As just mentioned, we will focus on correlation lengths ξ of mesonic observables, that is operators of the type $\mathcal{O} = \bar{\psi} \Gamma F^a \psi$, where

$$\Gamma = \{1, \gamma_5, \gamma_\mu, \gamma_\mu \gamma_5\}, \quad (1)$$

$$F^a = \{F^s, F^n\}, \quad F^s \equiv \mathbb{I}_{N_f \times N_f}, \quad F^n = \text{traceless } N_f \times N_f \text{ matrix}, \quad (2)$$

N_f is the number of quark flavours, and all colour, spinor and flavour indices have been suppressed. We may recall that at least some among these operators have direct physical significance, for instance

$$\bar{\psi} \gamma_5 F^s \psi \propto \eta' \text{-meson}, \quad (3)$$

$$\bar{\psi} \gamma_5 F^n \psi \propto \text{pion}, \quad (4)$$

$$\bar{\psi} \gamma_0 F^s \psi \propto \text{baryon number density}, \quad (5)$$

$$\bar{\psi} \gamma_0 F^n \psi \propto \text{electric charge density (for } N_f = 3 \text{)}. \quad (6)$$

The lattice determination of spatial correlation functions for operators of this type was pioneered by DeTar and Kogut¹⁰ and others¹¹ a long time ago, but quantitatively significant results relevant for the physical infinite volume chiral continuum limit, are only being produced presently.^{12–15} In order to streamline the discussion, we will restrict to one of the operators in the following, namely the interpolating field for the pion: $\pi \sim i \bar{\psi} \gamma_5 F^n \psi$. For $\bar{\psi} \gamma_0 F^s \psi$, see Sec. 4, and for the other operators, Ref. 9.

The spatial correlation function of the pion field has at large distances ($|\mathbf{x}| \rightarrow \infty$) the structure

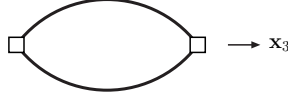
$$C_{\mathbf{x}} \equiv \int_0^{1/T} d\tau \langle \pi(\tau, \mathbf{x}) \pi(0, \mathbf{0}) \rangle \sim \frac{1}{|\mathbf{x}|^n} \exp\left(-\frac{|\mathbf{x}|}{\xi(T)}\right), \quad (7)$$

where τ is the Euclidean time coordinate of the imaginary time formulation. In Eq. (7), n is some unspecified power, while $\xi(T)$ defines the correlation length we are interested in. We will denote the inverse of the correlation length by $m \equiv \xi^{-1}$, and call it a “screening mass”.

The question now is, how does $m(T)$ behave as the temperature is increased from below to above the critical temperature T_c of the chiral phase

transition? At small temperatures, chiral symmetry is broken, and the pion is massless in the chiral limit, resulting in an infinite correlation length, or $m = 0$. At high temperatures, on the other hand, the screening mass approaches $2\pi T$, as we will recall presently. Thus the pion screening mass provides for a finite and gauge-invariant “order parameter” for chiral symmetry restoration.

The reason that the screening mass equals $2\pi T$ at high temperatures, is easily understood. For $T \gg T_c$, asymptotic freedom sets in, and the correlator can be determined in perturbation theory. A computation of the leading order graph,



and a subsequent Fourier transform [$C_{\mathbf{p}} = \int_{\tau, \mathbf{x}} \exp(-i\omega_n \tau - i\mathbf{p} \cdot \mathbf{x}) C_{\mathbf{x}}$], yield

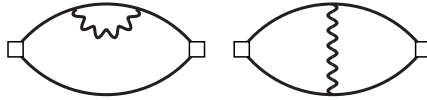
$$C_{\mathbf{p}} \sim \text{Tr}[F^n F^n] N_c T \sum_{n=-\infty}^{\infty} \frac{i|\mathbf{p}|}{8\pi} \ln \frac{2\omega_n - i|\mathbf{p}|}{2\omega_n + i|\mathbf{p}|}, \quad \omega_n = 2\pi T(n + \frac{1}{2}). \quad (8)$$

Now, the singularity closest to the origin in momentum space (determining the behaviour at the largest distances in configuration space) is seen to be a two-particle threshold at $|\mathbf{p}| = \pm 2i\omega_0$. Referring for a moment to the spatial directions in a (2+1)-dimensional language, with x_3 as the “time” coordinate, both quarks are on-shell at this point and have a minimal “energy” $ip_3 = \pm\omega_0$ [the minimal energy appears for a momentum $\mathbf{p}_{\perp} = \mathbf{0}$, where we denoted $\mathbf{p} \equiv (\mathbf{p}_{\perp}, p_3)$]. Thus, taking an inverse Fourier transform back to configuration space, we obtain the exponential decay advertised above, $C_{\mathbf{x}} \sim \exp(-2\omega_0|\mathbf{x}|)$.

3. Next-to-leading order for flavour non-singlet correlators

The question we would like to address next is, what is the first weak-coupling correction to $m = 2\pi T$? This computation has been described in Ref. 9, and we only reiterate the main steps here.

For flavour non-singlet operators, the relevant graphs might appear to be



but in fact there are infinitely many higher order graphs that need to be taken into account, symbolically of the types



These are not suppressed, because near the two-particle threshold, the quarks are almost on-shell, $p^2 = \omega_n^2 + \mathbf{p}_\perp^2 + p_3^2 \approx 0$, and consequently the dimensionless expansion parameter associated with adding a further line can be seen to be $\mathcal{O}(g^2 T/|\mathbf{p}|) \sim \mathcal{O}(1)$. In other words, the situation is analogous to the computation of the energy of a two-quark bound state at zero temperature, where again infinitely many graphs contribute.

The analogy with the bound-state system suggests immediately a tool for organising the computation: As in the study of quarkonia at $T = 0$, energies of bound states can be addressed with an effective theory called “Non-Relativistic QCD” (NRQCD).¹⁶ NRQCD techniques were first employed in the present context by Huang and Lissia.¹⁷

In order for an effective description to apply, the system must possess a scale hierarchy. Let us recall why one exists here, at high enough temperatures where the QCD coupling constant g is small. The basic point is that because quarks of a definite Matsubara frequency ω_n interact with bosonic Matsubara zero-modes only, we expect that their off-shellness is related to the momentum scales of the latter: $|ip_3 \pm \omega_n| \lesssim gT$. More precisely, we may recall that the static potential has in (2+1) dimensions the structure

$$V(\mathbf{x}_\perp) \sim g^2 T \ln |\mathbf{x}_\perp|. \quad (9)$$

Thus the typical (transverse) momentum \mathbf{p}_\perp of the bound-state constituents satisfies

$$\mathbf{p}_\perp^2 / \omega_n \sim V(\mathbf{x}_\perp) \Rightarrow \mathbf{p}_\perp^2 \sim (gT)^2, \quad (10)$$

and the binding energy is (dropping again possible logarithms)

$$|ip_3 \pm \omega_n| \sim \mathbf{p}_\perp^2 / \omega_n \sim V(\mathbf{x}_\perp) \sim g^2 T. \quad (11)$$

We thus indeed find a scale hierarchy

$$|ip_3 \pm \omega_n| \ll |\mathbf{p}_\perp| \ll \omega_n. \quad (12)$$

The effective action for this kinematic range can most easily be constructed by choosing a convenient basis for Dirac matrices (making $\gamma_0 \gamma_3$

diagonal), and rewriting then the Dirac spinor as

$$\psi \equiv \begin{pmatrix} \chi \\ \phi \end{pmatrix}, \quad (13)$$

where χ , ϕ are two-component spinors. In this basis the pion operator becomes $\pi \sim i(\chi^\dagger \sigma_3 \phi - \phi^\dagger \sigma_3 \chi)$, where σ_3 is a Pauli matrix. Restricting to the Matsubara mode ω_0 and expanding the QCD action to order $1/\omega_0$, the (on-shell) effective Lagrangian reads

$$\mathcal{L} = i\chi^\dagger \left(\omega_0 - gA_0 + D_3 - \frac{\nabla_\perp^2}{2\omega_0} \right) \chi + i\phi^\dagger \left(\omega_0 - gA_0 - D_3 - \frac{\nabla_\perp^2}{2\omega_0} \right) \phi, \quad (14)$$

where D_3 is a covariant derivative. We may note that:

- Both A_0 and A_3 play an important dynamical role.
- The transverse gauge fields A_1, A_2 , on the other hand, can be ignored, as long as we are interested in an energy shift of $\mathcal{O}(g^2T)$: they are of higher order than $\nabla_\perp \sim gT$. (They would be of order unity with respect to the magnetic scales $\nabla_\perp \sim g^2T$, but that gives an energy correction of order $\mathcal{O}(g^4T)$ only.)
- To be consistent at $\mathcal{O}(g^2T)$, we should replace ω_0 of the tree-level effective Lagrangian by a matching coefficient $M = \omega_0 + \mathcal{O}(g^2T)$ that needs to be determined.

While the final value of the matching coefficient M is unambiguous, there are many ways to determine it. In order to avoid computing wave function normalisation factors, we determine M by matching on-shell quark self-energies in the original QCD as well as in the effective theory of Eq. (14). On the side of QCD, a simple 1-loop graph,



produces near the pole the inverse propagator

$$\Sigma(p) = i\not{p} - ig^2 C_F \oint_q \frac{\gamma_\mu (\not{p} - \not{q})_f \gamma_\mu}{(p-q)_f^2 (q^2 + \lambda^2)_b} \Big|_{p^2=0}, \quad (15)$$

where $C_F = (N_c^2 - 1)/2N_c$, N_c is the number of colours, \oint is the standard imaginary-time integration measure, $(\dots)_f$ and $(\dots)_b$ denote fermionic and bosonic Matsubara four-momenta, respectively, and we have introduced a gluon mass λ as an intermediate infrared (IR) regulator. It can be seen

that the integral in Eq. (15) remains finite for $\lambda \rightarrow 0$, and then, up to order $\mathcal{O}(g^2)$, solving for the zero of Eq. (15) is equivalent to solving

$$p^2 + m_{\text{eff}}^2 = 0, \quad (16)$$

where $m_{\text{eff}}^2 = g^2 T^2 C_F / 4$ is nothing but the “hard effective mass” of quarks introduced recently in Ref. 18.

On the side of NRQCD, the computation of the quark self-energy is to be carried out order by order in $1/\omega_0$.¹⁹ It is easy to see that, in fact, 1-loop corrections then vanish,^a such that the on-shell point is determined directly by the mass scale M appearing in the tree-level propagator, $ip_3 = \pm M$.

Consequently, solving for the zeros in ip_3 of Eq. (16) to order $\mathcal{O}(g^2 T)$, we see that M needs to match $\omega_0 + m_{\text{eff}}^2 / 2\omega_0$, leading to

$$M = \omega_0 + g^2 T \frac{C_F}{8\pi} + \mathcal{O}(g^4 T). \quad (17)$$

This value replaces ω_0 in the first terms inside the parentheses in Eq. (14).

The parameters of the effective theory having been determined, it remains to solve its dynamics to order $g^2 T$. We define the correlation function

$$C(\mathbf{r}, x_3) \equiv \int_{\mathbf{R}} \left\langle \phi^\dagger \left(\mathbf{R} + \frac{\mathbf{r}}{2}, x_3 \right) \sigma_3 \chi \left(\mathbf{R} - \frac{\mathbf{r}}{2}, x_3 \right) \chi^\dagger(0) \sigma_3 \phi(0) \right\rangle, \quad (18)$$

and integrate out A_0, A_3 . To order $\mathcal{O}(g^2)$, $C(\mathbf{r}, x_3)$ satisfies the partial differential equation

$$\left[\partial_{x_3} + 2M - \frac{1}{\omega_0} \nabla_{\mathbf{r}}^2 + V(\mathbf{r}) \right] C(\mathbf{r}, x_3) \propto \delta(x_3) \delta(\mathbf{r}), \quad (19)$$

where

$$V(\mathbf{r}) = g^2 T C_F \int \frac{d^{2-2\epsilon} q}{(2\pi)^{2-2\epsilon}} \left\{ \frac{1 - e^{i\mathbf{q} \cdot \mathbf{r}}}{q^2 + \lambda^2} - \frac{1 + e^{i\mathbf{q} \cdot \mathbf{r}}}{q^2 + m_D^2} \right\} \quad (20)$$

$$= g^2 T \frac{C_F}{2\pi} \left[\ln \frac{m_D r}{2} + \gamma_E - K_0(m_D r) \right]. \quad (21)$$

On the last line we took the continuum limit ($\epsilon \rightarrow 0$) and removed the IR regulator from the propagator of A_3 ($\lambda \rightarrow 0$). Moreover, K_0 is a modified Bessel function, and m_D is the Debye mass appearing in the propagator of A_0 , $m_D^2 = g^2 T^2 (N_c/3 + N_f/6)$. Solving for the lowest energy level of the Schrödinger equation following from Eq. (19) at $x_3 \neq 0$, we finally obtain

$$m = 2\pi T + g^2 T \frac{C_F}{2\pi} \left(\frac{1}{2} + \hat{E}_0 \right), \quad \hat{E}_0^{N_f=0} = 0.164, \quad (22)$$

^aIt is important to note that at this point we are using un-resummed gluon propagators both on the QCD and on the effective theory side.

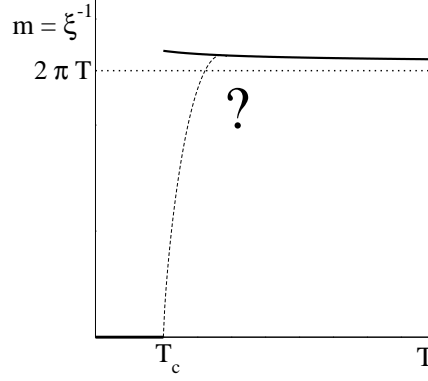


Figure 1. The pion screening mass as a function of the temperature. The dashed line is a guess for how the low- T and high- T limits might be connected, and in the continuous form drawn assumes a second order transition (i.e. $N_f = 2$). Note, however, that no sign of the indicated overshooting of $2\pi T$ has been observed in lattice simulations.

where \hat{E}_0 depends mildly on N_f (cf. Ref. 9), and we have shown explicitly the value relevant for the quenched theory.^b

Note that in Eq. (22), the factor $1/2$ inside the parentheses comes from the “constituent mass” correction in Eq. (17), while \hat{E}_0 comes from the solution of the Schrödinger equation. If the solution corresponds to a bound state, why then is \hat{E}_0 positive? The answer lies simply in the form of the potential in Eq. (21): it is a logarithmically “confining” potential, with $V(\mathbf{r} \rightarrow \mathbf{0}) \rightarrow -\infty$, $V(\mathbf{r} \rightarrow \infty) \rightarrow +\infty$, whose overall normalisation just happens to be such that the lowest energy eigenvalue is positive.

The result of Eq. (22) is plotted, with a certain choice of renormalisation scale for g^2 (cf. Ref. 3), in Fig. 1. We note that the correction appears small even at realistic T , but positive in sign. The change of m across T_c is thus very rapid — it is not smoothed by the $\mathcal{O}(g^2)$ term like for the pressure,²⁰ but rather made more pronounced. Close enough to T_c the mass of course has to decrease, either continuously (the case for $N_f = 2$, indicated with a dashed line in Fig. 1), or with a small discontinuity (for $N_f = 0, 3$).

For the pressure, the next-to-next-to-leading order correction, $\mathcal{O}(g^3)$, comes with an opposite sign to $\mathcal{O}(g^2)$, and appears very large.²¹ (At the same time the ultimate result, including higher orders still,²² resembles

^bTo be precise, the quenched theory value applies in the “perturbative” broken $Z(N_c)$ vacuum, i.e. the one where the phase of the Polyakov loop is trivial. In the unquenched theory this vacuum constitutes in any case the global ground state of the system.

more the $\mathcal{O}(g^2)$ approximation.) It would be interesting to find out whether there is an $\mathcal{O}(g^3)$ correction in the pion correlation length as well.

4. Flavour-singlet correlators

For flavour singlets the pattern is very different from the flavour non-singlets, as the singlet operators couple to purely gluonic “glueball” states. For baryon density, for instance, one finds that^{8,23}

$$\bar{\psi}\gamma_0 F^s \psi \longleftrightarrow -\frac{iN_f}{3\pi^2} g^3 \text{Tr}[A_0^3], \quad (23)$$

or graphically, that the correlation function is dominated by graphs like



The corresponding screening mass has been determined some time ago,⁸ and evaluates to $m(\text{Tr}[A_0^3]) \approx 5T$ at $T \approx 2T_c$. The inverse, $\xi \approx 1/5T$, is then the distance scale at which fluctuations in baryon number density are correlated. The glueball operators mediating the correlations of a number of other mesonic flavour-singlets have been worked out in Ref. 9.

5. On $U_A(1)$ symmetry at high temperatures

The $U_A(1)$ axial symmetry is broken explicitly by the anomaly. It has been suggested,²⁴ however, that it might get “effectively restored” somewhat above the critical temperature, say at $T \gtrsim 2T_c$. What is meant by this is that the topological susceptibility, $\chi = \langle \nu^2 \rangle / V$, where ν is the topological charge of the gauge configuration, or the net number of zero-modes of the Dirac operator, and V is the volume, decreases rapidly at temperatures above T_c . This becomes quite obvious particularly if the number of colours is increased above $N_c = 3$; see, e.g., Ref. 25 and references therein. Consequently, it could be expected that anomalous effects cease to operate.

It may be appropriate to remark at this point, though, that it is possible to find observables for which the $U_A(1)$ symmetry appears not to get restored. Consider, for instance, the screening masses for the operators $V_3^s = \bar{\psi}\gamma_3\psi$, $A_3^s = \bar{\psi}\gamma_3\gamma_5\psi$, measured from correlation functions in the x_3 -direction. Now, $U_A(1)$ symmetry restoration would imply that the correlation functions for V_3^s, A_3^s are identical and, therefore, that the screening masses are identical. Yet, a perturbative analysis can be used to indicate⁹

that A_3^s couples to the glueball-like state $g^2 \epsilon_{ij3} \text{Tr}[A_0 F_{ij}]$ of the dimensionally reduced theory,²⁶ and has thus a non-vanishing screening mass $m = m_D + \mathcal{O}(g^2 T)^{2,3}$ where the next-to-leading order correction is also known numerically.⁵ At the same time, the correlator related to V_3^s is exactly conserved, and has no non-trivial screening mass associated with it. Therefore, the $U_A(1)$ symmetry appears broken even at high temperatures.

6. Conclusions

Various mesonic correlation lengths are well-defined gauge-invariant physical observables that seem to be computable, for flavour non-singlets, at least up to next-to-leading order in the gauge coupling g^2 , as outlined in this talk. Higher orders could also be reached in principle. For flavour singlets, on the other hand, the correlation lengths can be related to those of purely gluonic states, which have been determined previously from the dimensionally reduced theory with good numerical precision.^{4,5,8}

The comparison of these analytic predictions with results from four-dimensional lattice simulations poses an interesting puzzle. Indeed, lattice results so far are consistent with the leading order value $m = 2\pi T$, as soon as the temperature is a bit above the critical one,^{12–15} while the next-to-leading order correction advertised above is positive, requiring an “overshooting” of $m = 2\pi T$. Lattice results involve systematic errors, though, so that the discrepancy cannot be considered too serious at present.

On the side of analytic efforts, one could envisage a number of computations which might facilitate the comparison with ever more precise future simulations. For instance, the leading discretization effects could be determined analytically, even though this of course is specific to the fermion action used. (Different groups have rather different preferences here.) Another point of possible relevance is that some of the correlation functions involve an x_3 -dependent prefactor in front of the exponential, and it might be useful to take it into account in the fitting procedure.

To conclude, let us recall that the ultimate theoretical goal of the exercise discussed here is to estimate the reliability of perturbation theory at finite T , in order to then use perturbation theory with more confidence for other observables for which lattice is not well suited. Given that good QCD predictions can eventually be obtained for static correlation lengths and that there is a remarkably stark difference between the two phases, one is however also lead to wonder, once again, whether some interesting phenomenological signatures might be found for these quantities.

Acknowledgments

I wish to thank M. Vepsäläinen for collaboration on the work presented in this talk, and S. Datta, E. Laermann, G.D. Moore and R.D. Pisarski for useful comments related to topics covered in it.

References

1. L.D. McLerran and T. Toimela, *Phys. Rev.* **D31**, 545 (1985).
2. P. Arnold and L.G. Yaffe, *Phys. Rev.* **D52**, 7208 (1995).
3. K. Kajantie *et al*, *Nucl. Phys.* **B503**, 357 (1997).
4. M.J. Teper, *Phys. Rev.* **D59**, 014512 (1999).
5. M. Laine and O. Philipsen, *Phys. Lett.* **B459**, 259 (1999); A. Hart and O. Philipsen, *Nucl. Phys.* **B572**, 243 (2000).
6. O. Kaczmarek *et al*, *Phys. Rev.* **D62**, 034021 (2000).
7. S. Datta and S. Gupta, *Phys. Lett.* **B471**, 382 (2000); *Phys. Rev.* **D67**, 054503 (2003).
8. A. Hart, M. Laine and O. Philipsen, *Nucl. Phys.* **B586**, 443 (2000); *Phys. Lett.* **B505**, 141 (2001).
9. M. Laine and M. Vepsäläinen, *JHEP* **02**, 004 (2004).
10. C. DeTar and J.B. Kogut, *Phys. Rev. Lett.* **59**, 399 (1987); *Phys. Rev.* **D36**, 2828 (1987).
11. K.D. Born *et al*, *Phys. Rev. Lett.* **67**, 302 (1991).
12. P. de Forcrand *et al.*, *Phys. Rev.* **D63**, 054501 (2001).
13. E. Laermann and P. Schmidt, *Eur. Phys. J.* **C20**, 541 (2001).
14. R.V. Gavai, S. Gupta and R. Lacaze, *Phys. Rev.* **D65**, 094504 (2002); R.V. Gavai and S. Gupta, *Phys. Rev.* **D67**, 034501 (2003).
15. For a review and references, see E. Laermann and O. Philipsen, *Ann. Rev. Nucl. Part. Sci.* **53**, 163 (2003), and E. Laermann, these proceedings.
16. W.E. Caswell and G.P. Lepage, *Phys. Lett.* **B167**, 437 (1986).
17. S. Huang and M. Lissia, *Nucl. Phys.* **B480**, 623 (1996).
18. P. Arnold, G.D. Moore and L.G. Yaffe, *JHEP* **01**, 030 (2003).
19. A.V. Manohar, *Phys. Rev.* **D56**, 230 (1997).
20. E.V. Shuryak, *Sov. Phys. JETP* **47**, 212 (1978); S.A. Chin, *Phys. Lett.* **B78**, 552 (1978).
21. J.I. Kapusta, *Nucl. Phys.* **B148**, 461 (1979).
22. K. Kajantie *et al*, *Phys. Rev.* **D67**, 105008 (2003); *JHEP* **04**, 036 (2003); A. Vuorinen, *Phys. Rev.* **D68**, 054017 (2003).
23. D. Bödeker and M. Laine, *JHEP* **09**, 029 (2001).
24. E.V. Shuryak, *Comm. Nucl. Part. Phys.* **21**, 235 (1994); G. Boyd *et al*, hep-lat/9607046; J.B. Kogut, J.F. Lagae and D.K. Sinclair, *Phys. Rev.* **D58**, 054504 (1998); S. Chandrasekharan *et al*, *Phys. Rev. Lett.* **82**, 2463 (1999).
25. B. Lucini, M. Teper and U. Wenger, hep-lat/0401028; L. Del Debbio, H. Panagopoulos and E. Vicari, hep-th/0407068.
26. P. Ginsparg, *Nucl. Phys.* **B170**, 388 (1980); T. Appelquist and R.D. Pisarski, *Phys. Rev.* **D23**, 2305 (1981).